QPT 2025

Guilin, China

Updates on Experimental Search for CME

Jinhui Chen

Fudan University

24-28, October

Outline

- Introduction
- STAR Isobar results
- STAR BES-II results with Event Shape Selection
- Updates from 200 GeV and LHC energies
- Summary and Outlook

The Chiral Anomaly

- ABJ anomaly determines the violation of chiral symmetry when massless fermions are coupled to an abelian gauge field.

$$\partial_\mu J^\mu_A \propto < {}^*F^{\mu\nu} F_{\mu\nu} > \qquad (1.1)$$

J. Bell, R. Jackiw, Nuovo Cim. A 60, 47 (1969)

$$\partial^\mu j^5_\mu(x) = 2im_0 j^5(x) + \frac{\alpha_0}{4\pi} F^{\xi\sigma}(x) F^{\tau\rho}(x)\epsilon_{\xi\sigma\tau\rho} \quad , \qquad (1)$$

S. Adler, Phys. Rev. 177, 2426 (1969)

R. Jackiw, arXiv:0403109; S. Adler, arXiv:0405040; at ”50 years of Yang-Mills theory”

- Tabletop exps. observed the chiral anomaly through the studies of magnetotransport in Dirac and Weyl semimetals.

“In parallel electric and magnetic fields, charge is predicted to flow between the Weyl nodes, leading to negative magnetoresistance.”

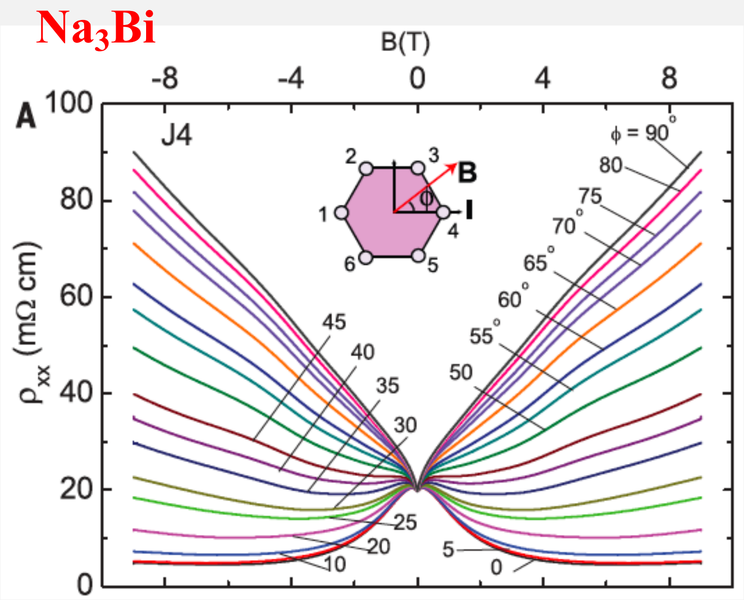

J. Xiong et al., Science 350, 413 (2015);

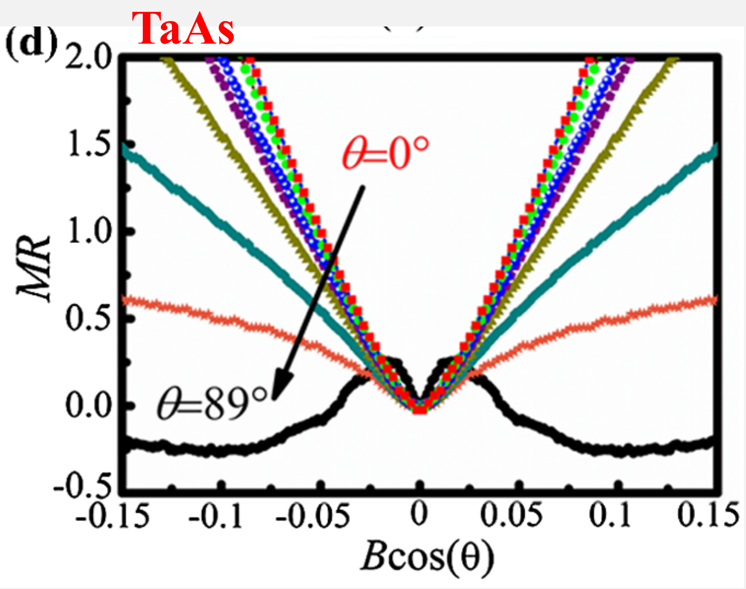

X. Huang et al., Phys. Rev. X 5, 031023 (2015);

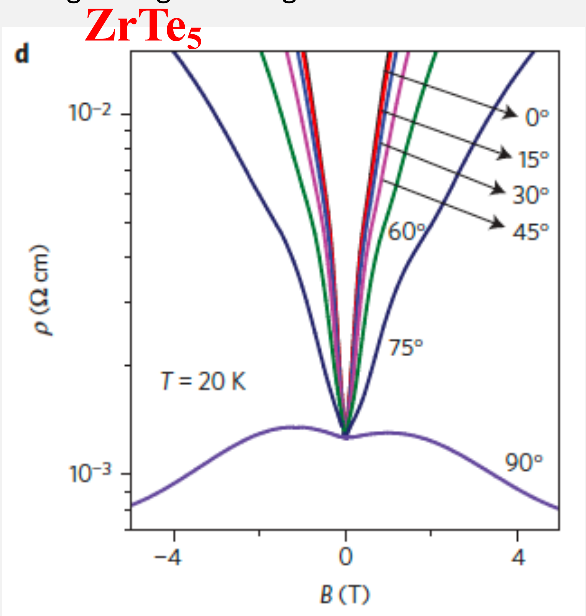

Q. Li et al., Nat. Phys. 12, 550 (2016)

Chiral Anomaly in Heavy-Ion Collisions

- Chiral Magnetic Effect: Chirality imbalance of massless quarks coupled with strong magnetic field induces a charge separation along the B field direction, which violates local ***P*** and ***CP*** Symmetry in strong interaction.

D. Kharzeev, R. Pisarski, M. Tytgat, Phys. Rev. Lett. 81, 512 (1998); K. Fukushima, D. Kharzeev, H. Warringa, Phys. Rev. D 78, 074033 (2008)…

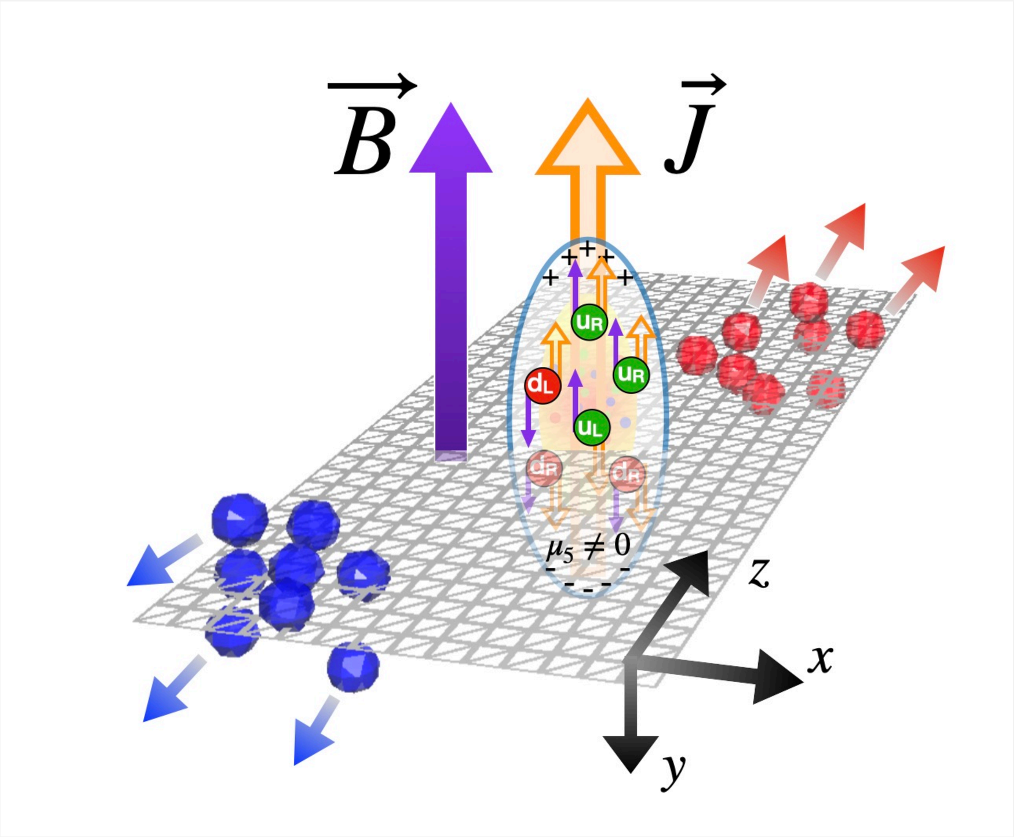

STAR arXiv:2506.00275

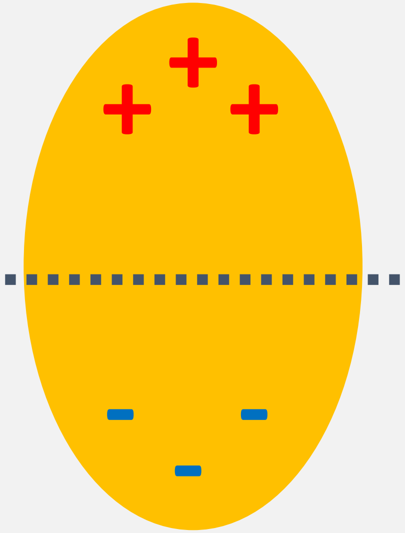

Chiral Magnetic Effect (CME)

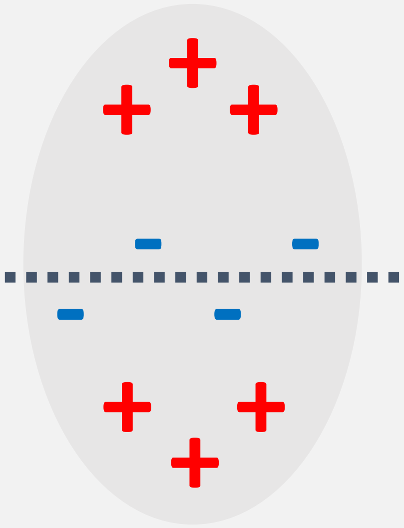

Chiral Magnetic Wave (CMW)

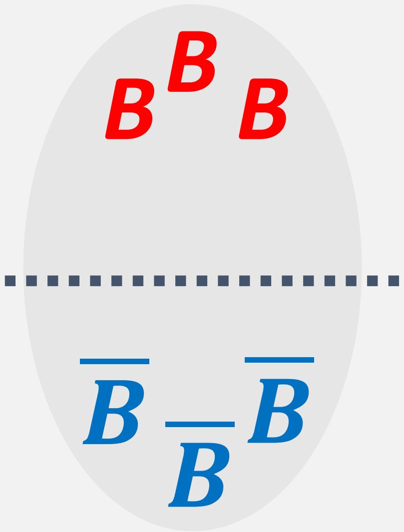

Chiral Vortical Effect (CVE)

The Isobar Program for CME Search

- One approach is to look for signal difference in controlled experiment of two isobars:

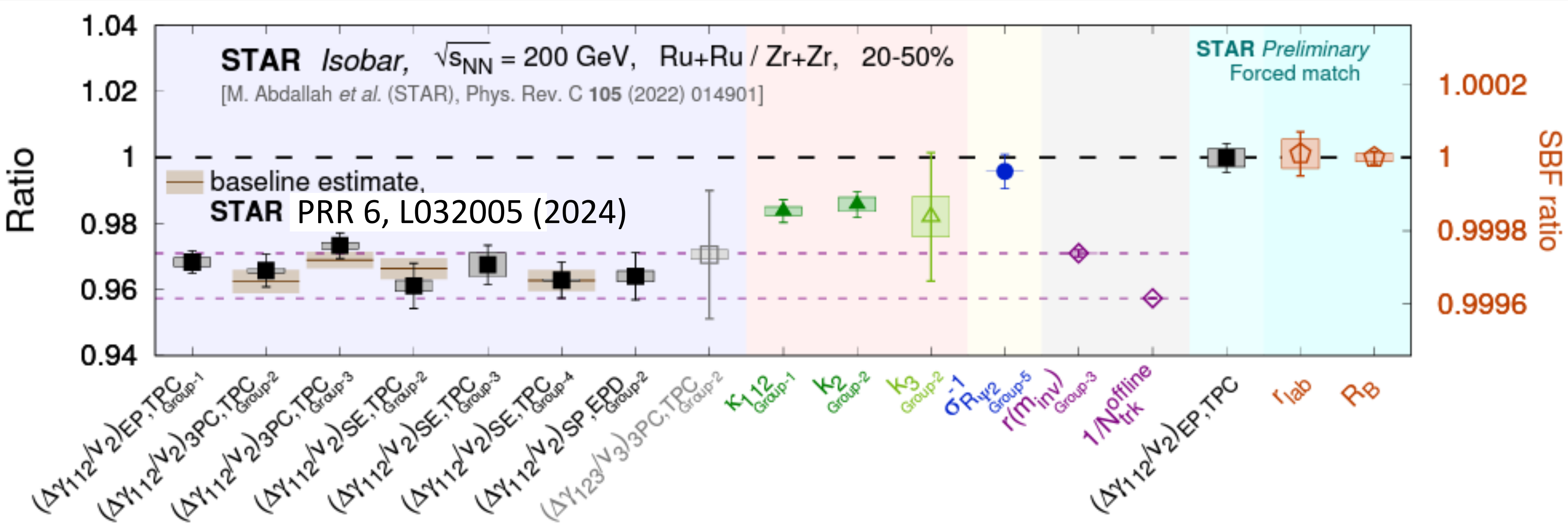

$$\gamma^{112} = \langle \cos(\varphi_1 + \varphi_2 - 2\Psi_{\mathrm{RP}}) \rangle$$

$$\Delta\gamma^{112} = \gamma_{OS}^{112} - \gamma_{SS}^{112}$$

S. Voloshin, Phys. Rev. C 70, 057901 (2004)

$$\frac{\Delta\gamma^{112}}{v_2} \rightarrow Ru + Ru > Zr + Zr$$

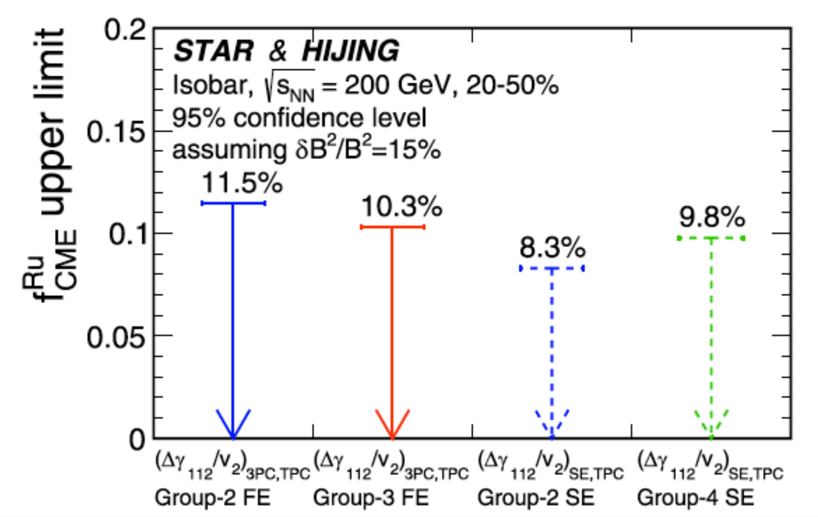

Important points from Isobar analysis:

- **Signal difference is too small to be detected via system's ΔZ.**
- **Background is significant: nuclear shape uncertainties limit the background accuracy no better than sub-percentage level.**

Improve the BKG suppression: ESS

- Large e-by-e fluctuations could dominate the observable:
  - participant zone geometry: expected to be long ranged in rapidity emission
  - pattern fluctuations: more localized, less correlated over rapidity

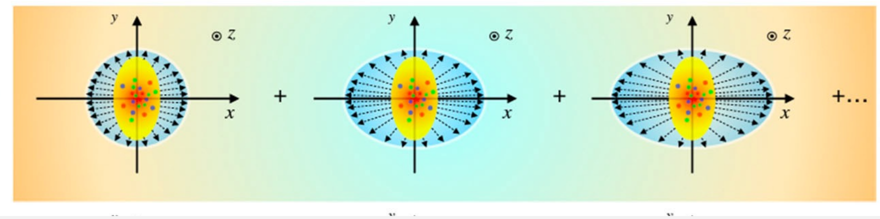

- Event shape variables based on particles of interest (POI) are sensitive to both geometry and emission pattern

H. Petersen and B. Muller, Phys. Rev. C 88, 044918(2013); Z. Xu et al, Phys. Lett. B 848,138367(2024)

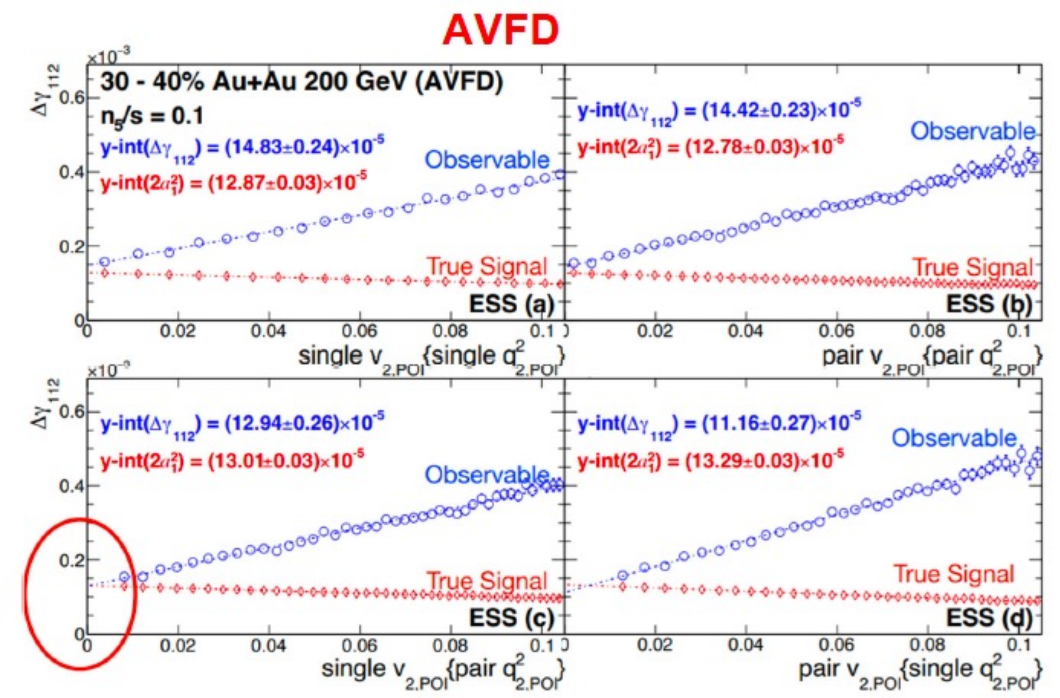

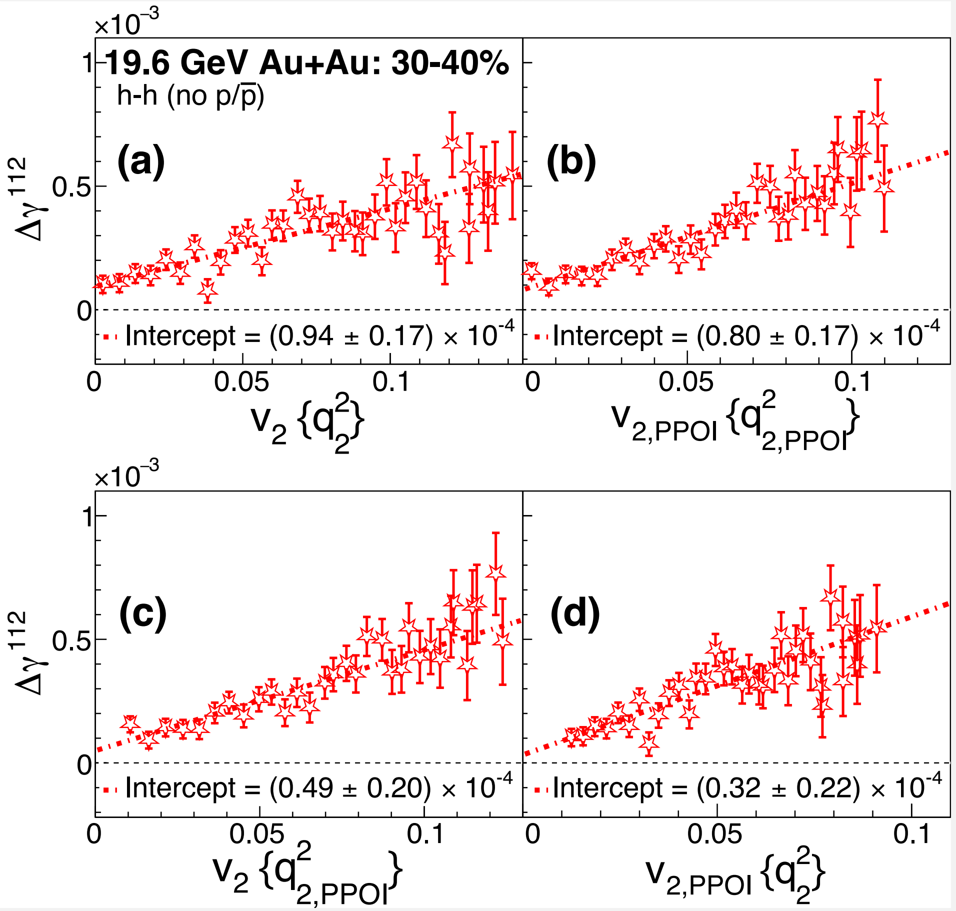

STAR arXiv:2506.00278

- Event Shape Selection (ESS) found that recipe (c) accurately matches the input CME signal.
- Intercepts follow an ordering (a)>(b)>(c)>(d).

Application to Data

BES-I

$\sqrt{S_{NN}}$(GeV)	Events (10^6)	Year
62.4	46	2010
39	86	2010
27	30	2011
19.6	15	2011
14.6	13	2014
11.5	7	2010
9.2	0.3	2008
7.7	4	2010

“Events” represents good events after quality cuts.

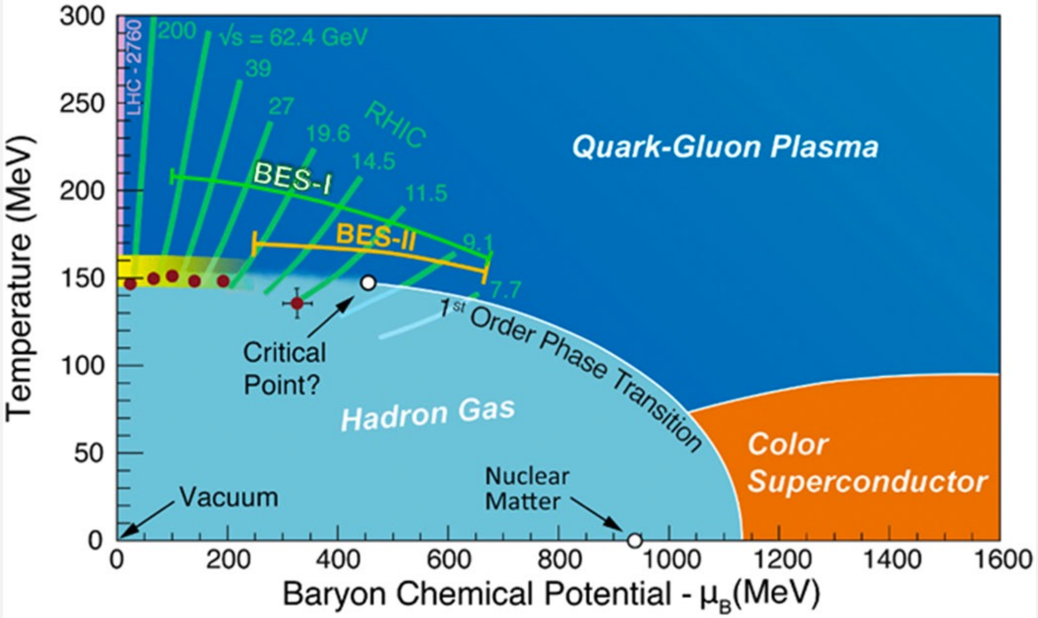

BES-II

$\sqrt{S_{NN}}$(GeV)	Events (10^6)	Year
27	555	2018
19.6	478	2019
14.6	324	2019
11.5	230	2020
9.2	160	2020
7.7	101	2021

Event Shape Selection **Spectator Ψ_1**

$$\Delta\gamma^{112} = \Delta\gamma^{CME} + k\cancel{\frac{v_2}{N}} + \cancel{\Delta\gamma^{non-flow}}$$

Measured **Signal** **Backgrounds**

$\eta > y_{beam}$: Forward spectators

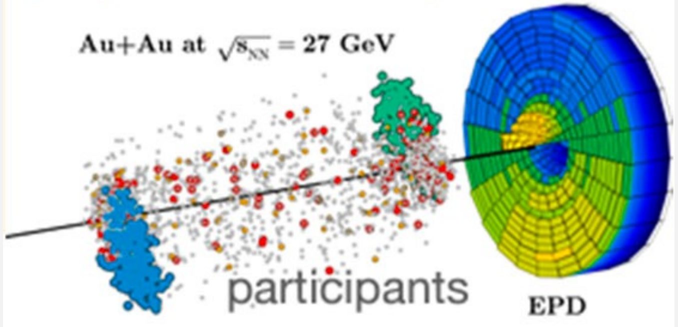

The Event Plane Detector at STAR

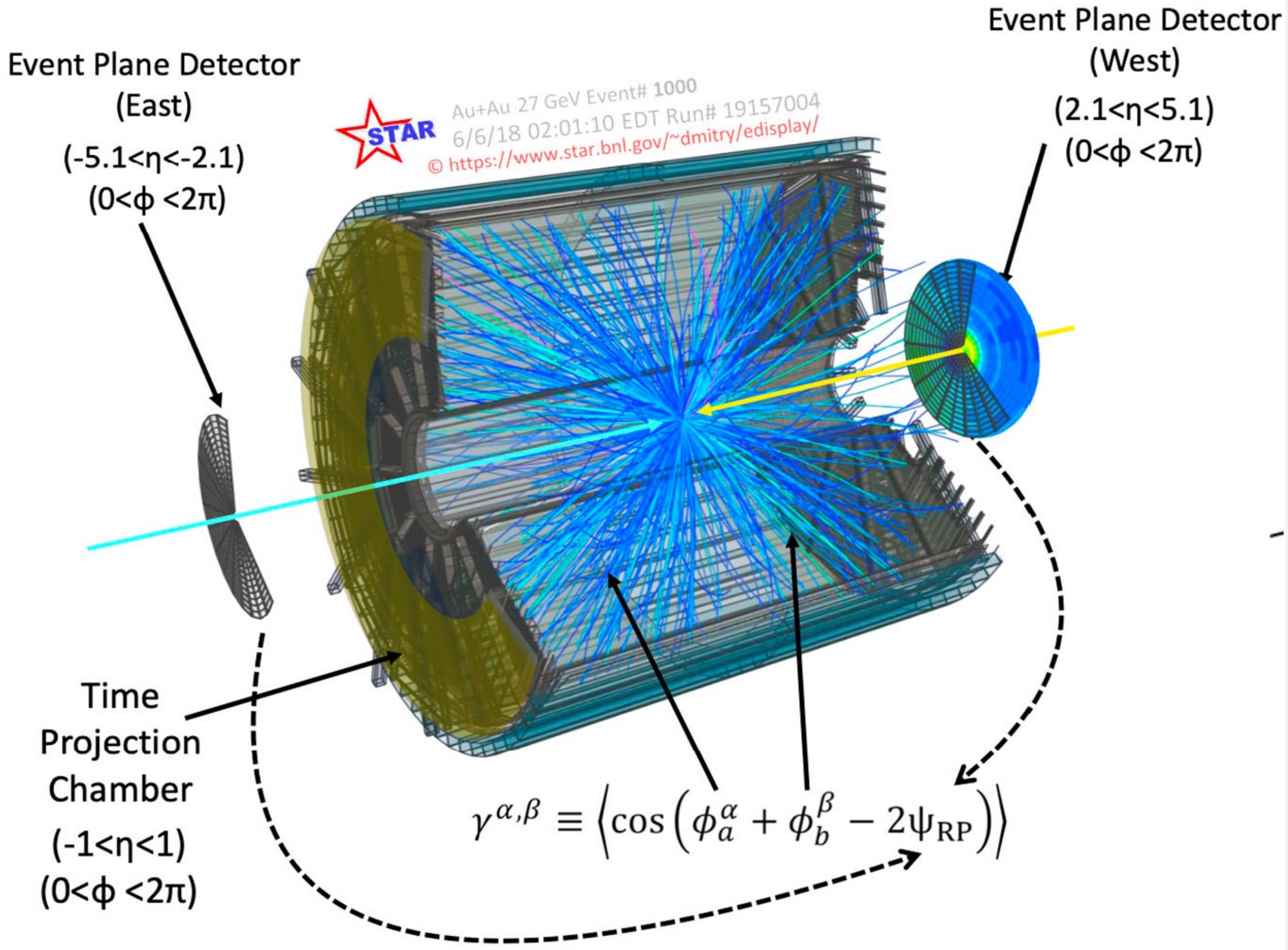

$$\gamma^{\alpha,\beta} \equiv \left\langle \cos\left(\phi_a^{\alpha} + \phi_b^{\beta} - 2\psi_{RP}\right)\right\rangle$$

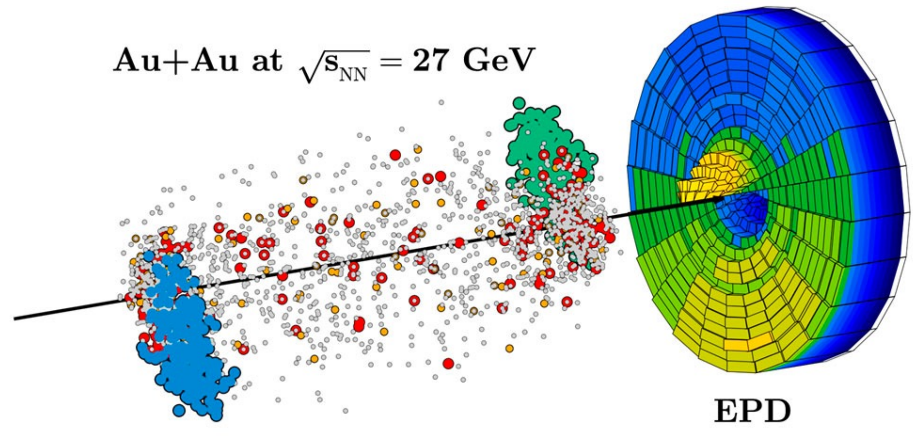

- ➢ Higher resolution, BES-II new detector (EPD)
- upgraded in 2018
- The inner EPD detects first-order spectator plane
- Targeting the spectator regions for B field
- Suppressing non-flow background

EPD for spectator proton plane measurement works for low beam energies.

Results of 27 GeV with EPD

STAR Phys. Lett. B 839, 137779 (2023)

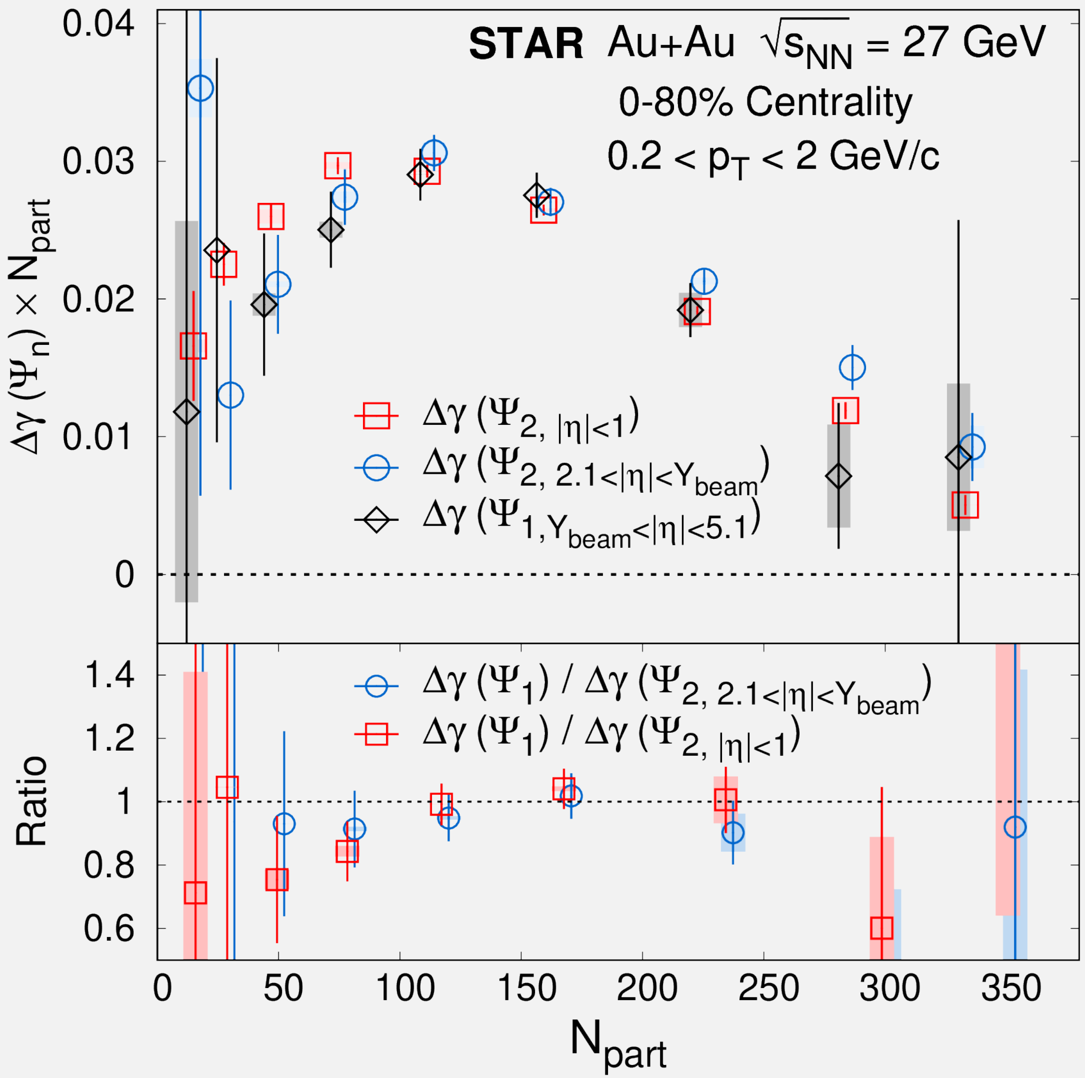

- The CME scenario is expected to result in a larger correlation relative to Ψ_1 than to Ψ_2, while a flow driven background scenario would lead to a consistent result for both event planes.
- Within current statistics, the magnitudes for different planes are consistent with each other.
- In 10-50% mid-central collisions, upper limits of ~10% using different planes.

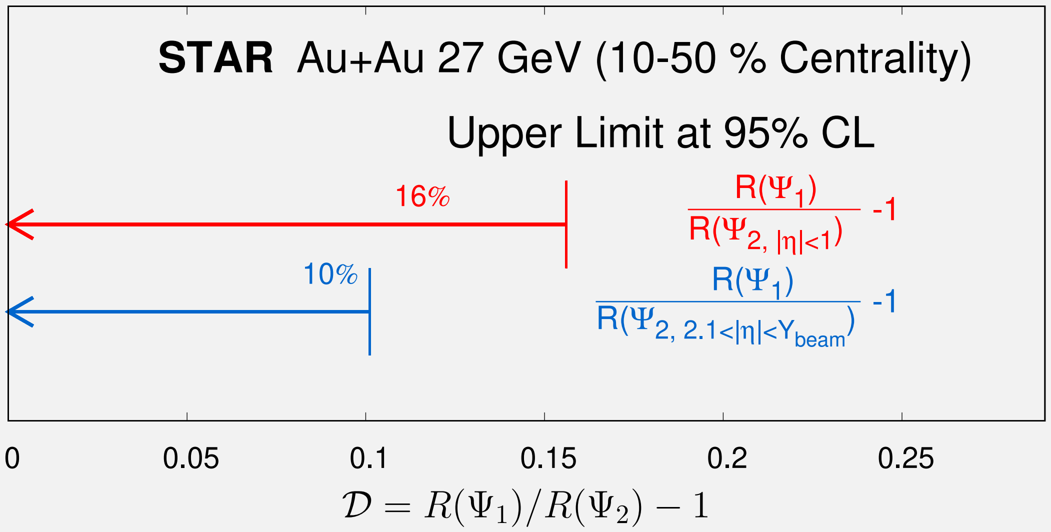

Results of BES-II Data with ESS

- We show the data of 19.6 GeV for this talk. Details of different energies can be found in 'STAR arXiv:2506.00278'

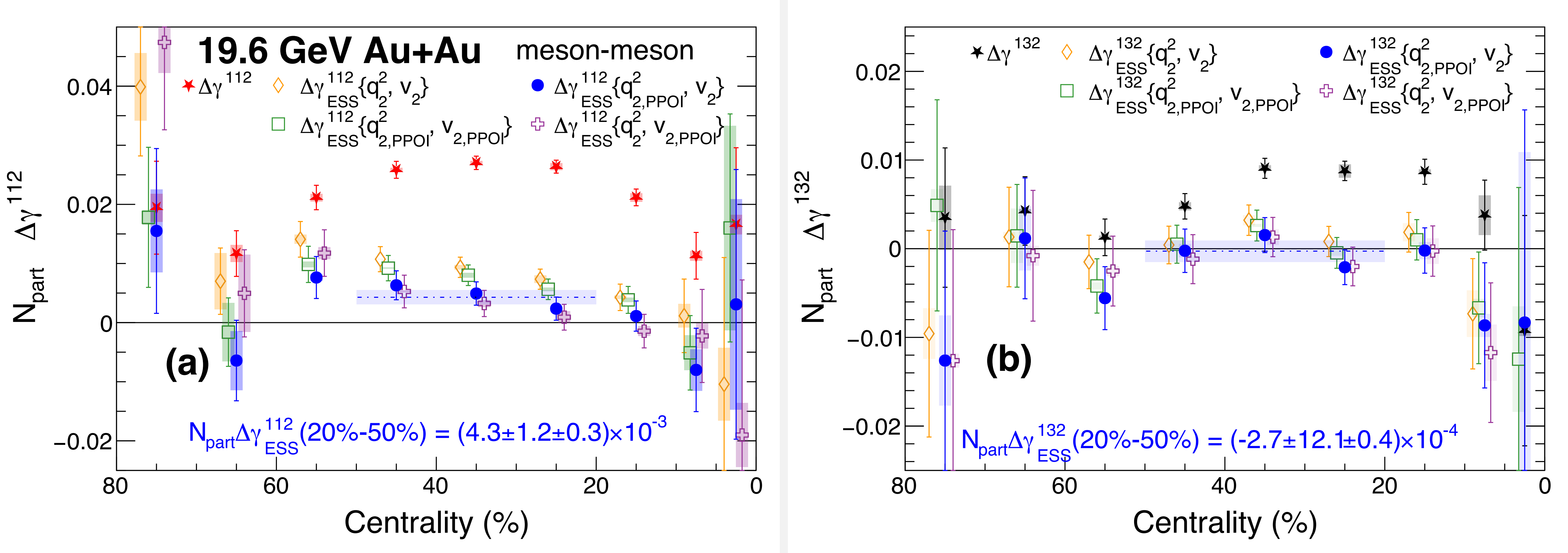

STAR arXiv:2506.00278

- After v_2-BKG subtraction, a finite signal in mid-central events with the optimal ESS (c), the blue filled points, a 3σ significance for 20%-50% centrality
- For BKG indicator $\Delta\gamma^{132}$, ESS results are consistent with zero – v_2-BKG suppressed

Results of BES-II Data with ESS (cont.)

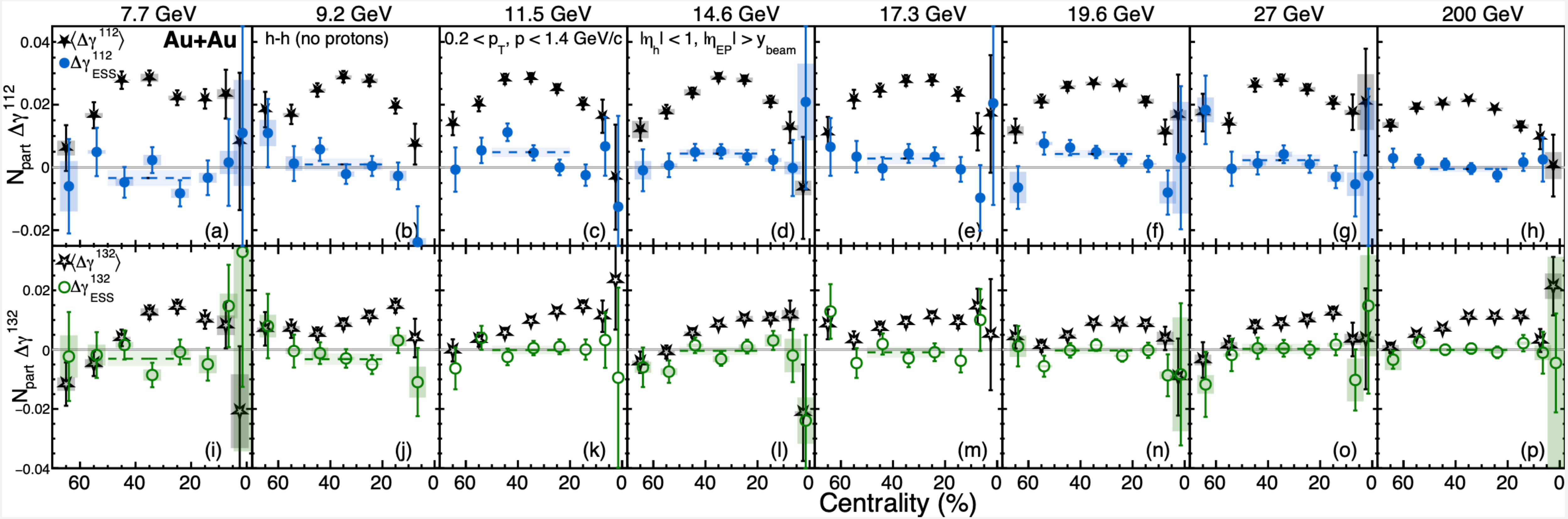

STAR arXiv:2506.00275, 2506.00278

- Residual charge separation $\Delta\gamma^{112}_{ESS}$ after suppressing BKG:
  - Finite (>3σ) at each of 19.6, 14.6 and 11.5 GeV
  - Zero at 200 GeV or below 10 GeV
- Background indicator $\Delta\gamma^{132}_{ESS}$ consistent with zero

Results of BES-II Data with ESS (cont. 2)

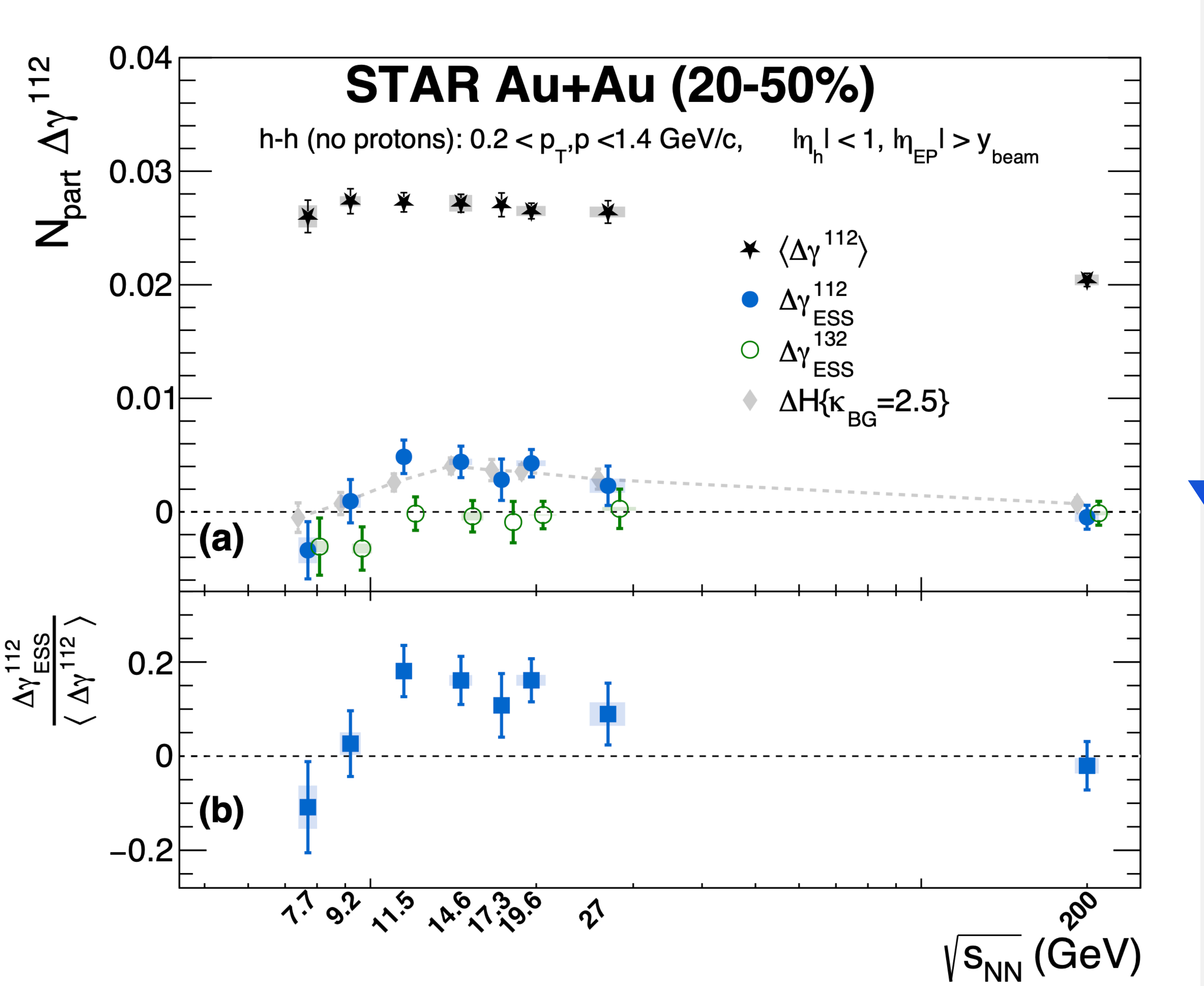

v_2-BKG suppressed by a factor of 4-5

- **Rise-and-fall beam energy trend: B field effect + life time of QGP?**
- **Why "sweet-zone" at 10-30 GeV?**

STAR arXiv:2506.00275, 2506.00278

Understand the Collision Energy Dependence

Kharzeev's slide @ Chirality 2025

ICTP-SAIFR, Sao Paulo, Brazil,
July 7-11, 2025

Why CME at low energies?

One reason is the **longer-living magnetic field** B.

Several effects combine to increase the lifetime of B at low energies:

Super Strong Magnetic Fields Leave Imprint on Nuclear Matter

Data from heavy ion collisions give new insight into electromagnetic properties of quark-gluon plasma

February 23, 2024

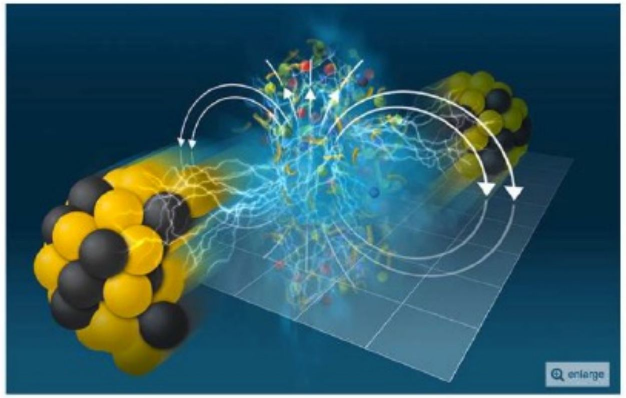

1. Slower spectator protons (kinematics)

2. Stronger stopping of electric charge

3. Stronger Faraday effect in a conducting plasma,
   increase of electric conductivity with the chemical potential

21

The Energy Dependence of Magnetic Field

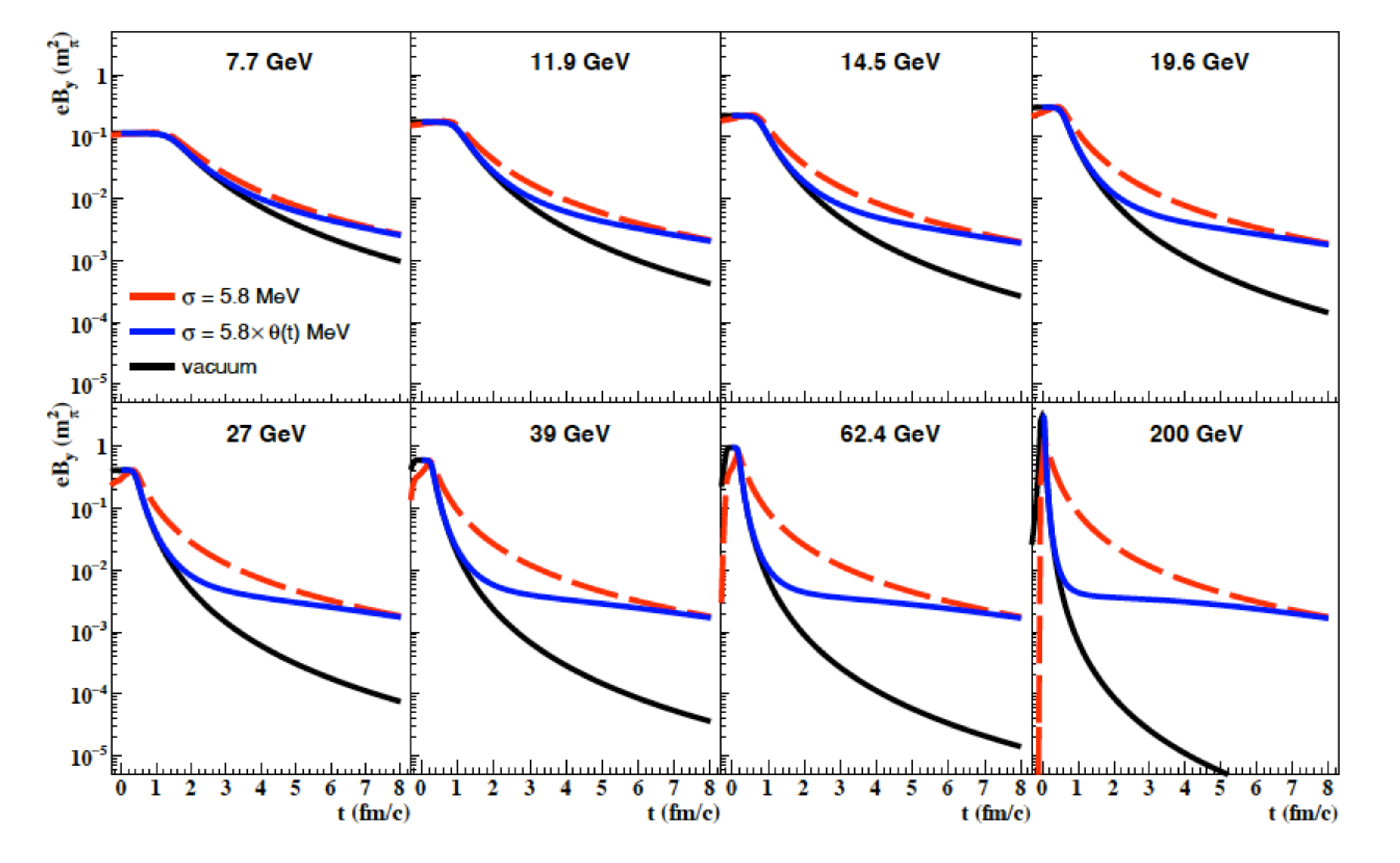

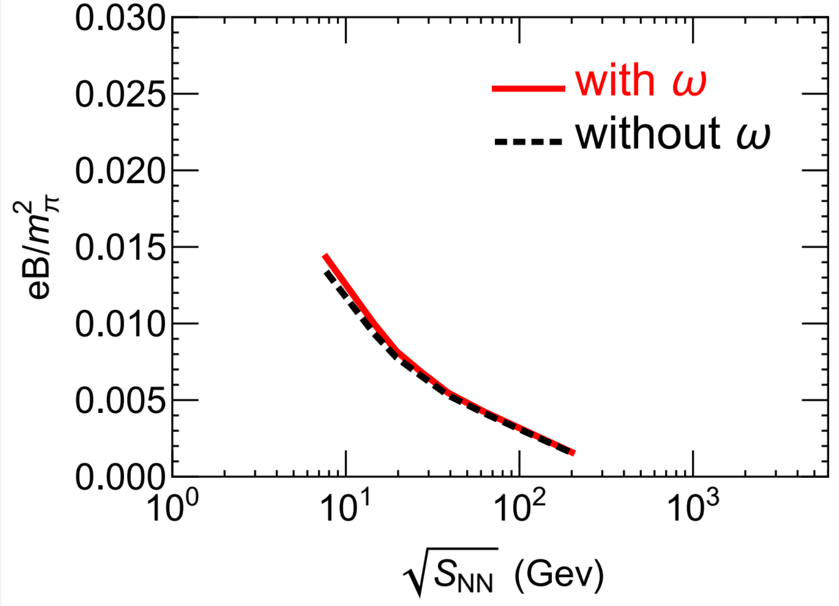

H. Li, X. Xia, X. Huang, H. Huang, Phys. Rev. C 108, 044902 (2024)
A. Huang, X. Wu, M. Huang, Phys. Rev. D 110, 094032 (2024)

- The longer-living magnetic field at lower energies; the strength of the late-state magnetic field is higher at lower energies regardless of the vorticity effect.

Imprint of Magnetic Field in QGP

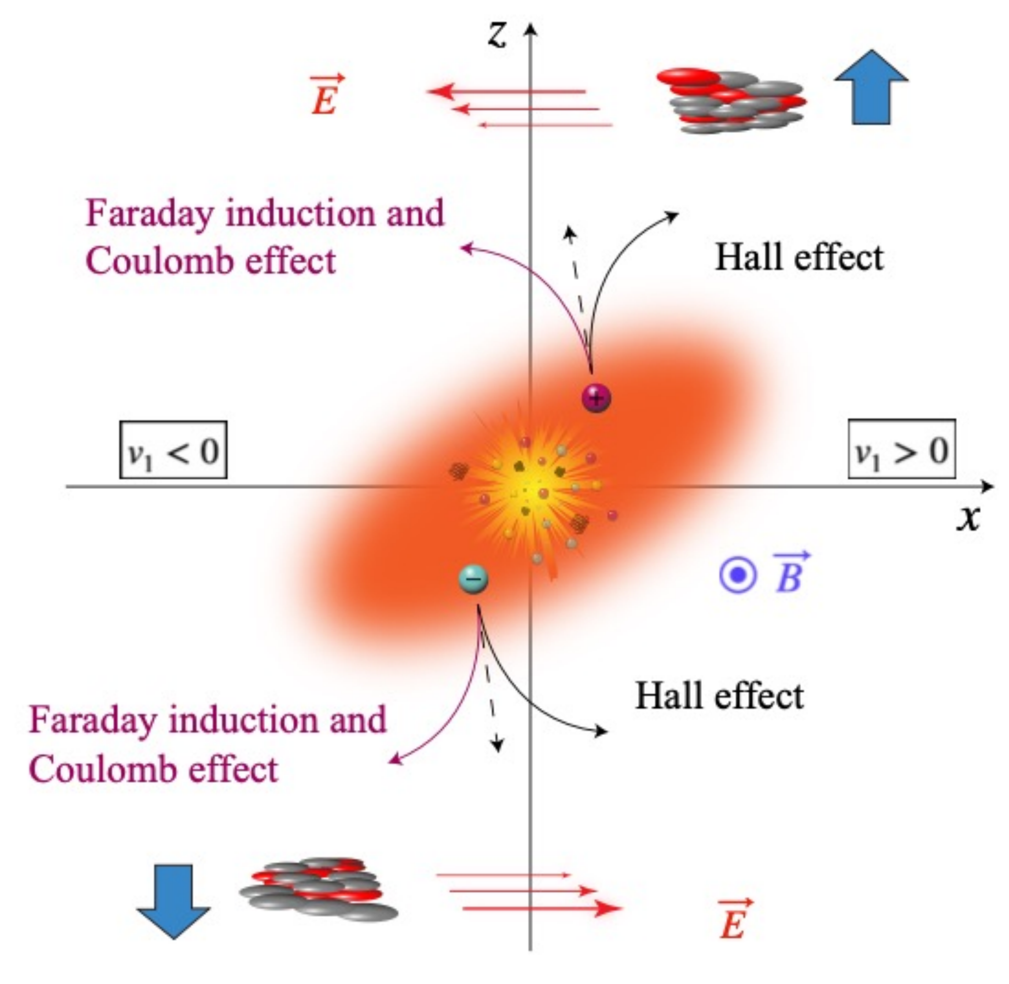

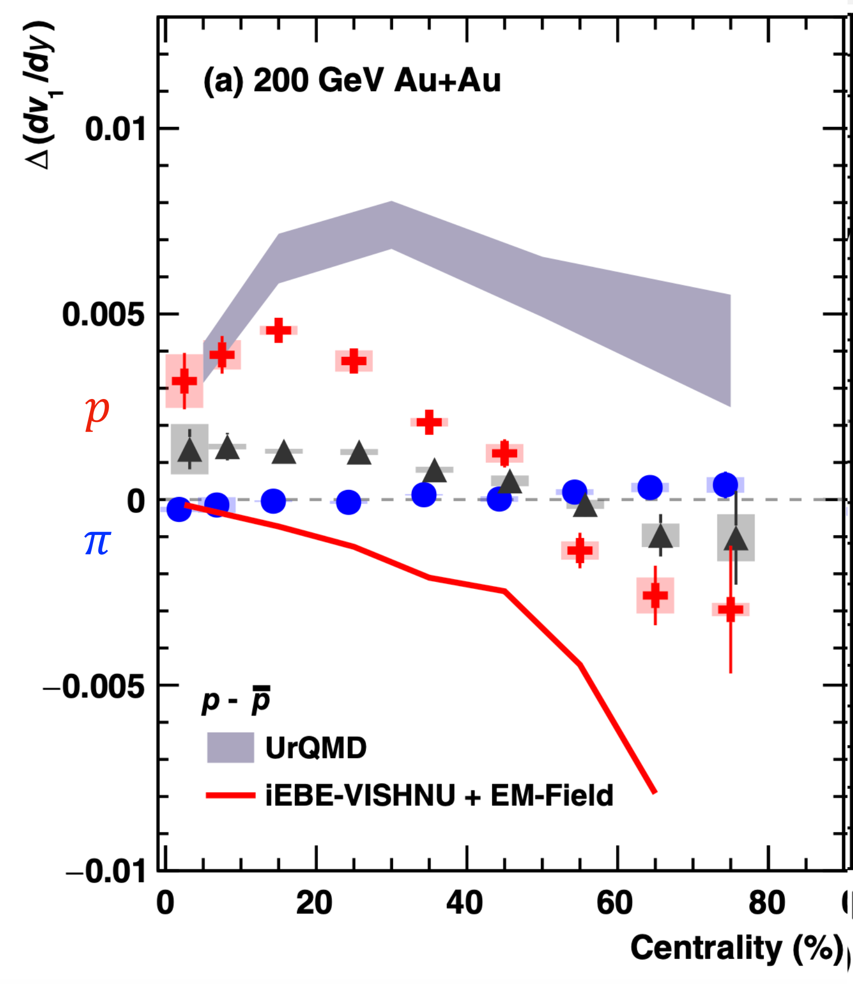

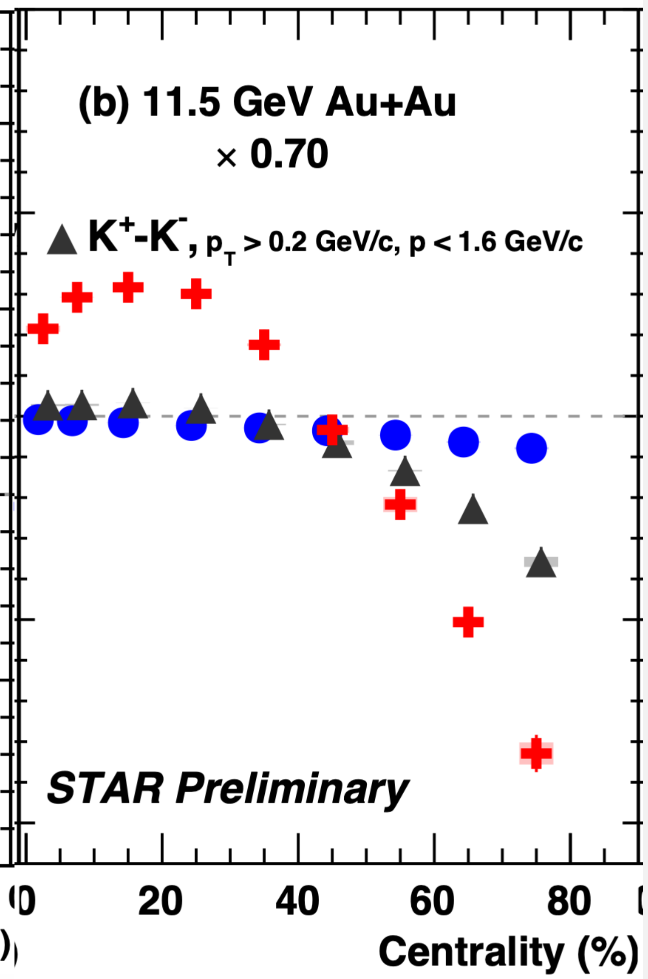

STAR, Phys. Rev. X 14, 011028 (2024); Feature in Physics, S. Chen, Physics.17.31 (2024)

- STAR observed the splitting of charged particle v_1 slope, imprint of B field on QGP, stronger at lower energy in RHIC BES-data

CME and B-field, Critical Point

- Holographic studies of CME by incorporating a time-dependence B-field found that the integrated chiral magnetic current exhibits a nonmonotonic dependence on the collision energy.
- The enhancement of topological fluctuations near the critical point revealed through real-time quantum simulations.
- Dynamical approach towards critical region?

S. Crueninger, S. M-Tejera, P. Romeu, Phys. Rev. D 112, 036003 (2025)

K. Ikeda, D. Kharzeev, Y. Kikuchi, Phys. Rev. D 103, L071502 (2021)

W. Zhou, H. Liu, F. Li, Y. Sun, J. Xu, C. Ko, Phys. Rev. C 104, 044901 (2021)

$$2\kappa^2 J_{\mathrm{CME}}^{\text{quasi-eq}} = 8\alpha\mu_5(\tau)B_z(\tau), \qquad (1.1)$$

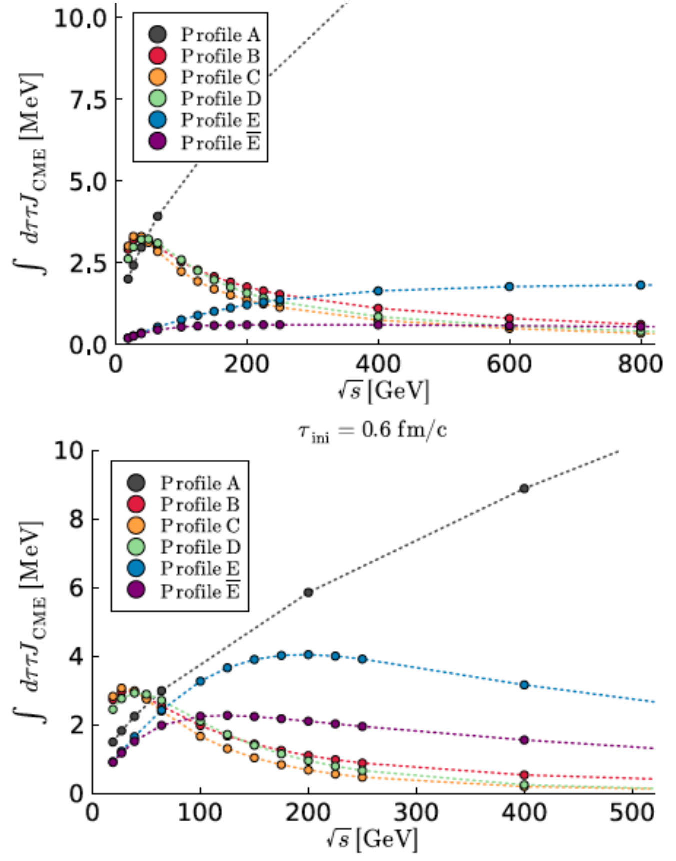

$$\frac{\chi_{\mathrm{CS}}}{g^2} = \frac{N-1}{\pi^2}\mathrm{Re}\int_0^{\hat{T}} d\hat{t}(t)\left(\langle \bar{L}(t)\bar{L}(0)\rangle - \langle \bar{L}(0)\rangle^2\right). \qquad (18)$$

$$L_n = \sum_{i=1}^{n}\left(\chi_i^\dagger\chi_i - \frac{1-(-1)^i}{2}\right), \qquad (11)$$

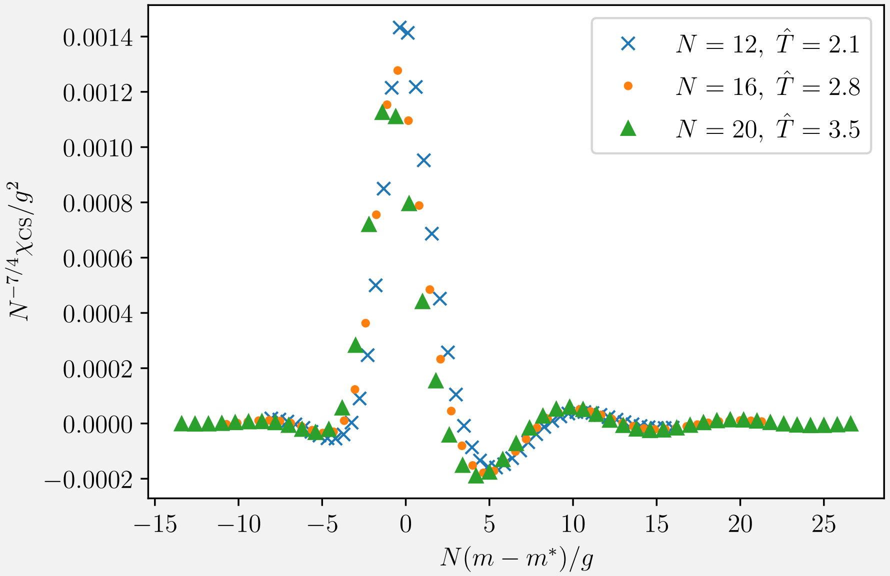

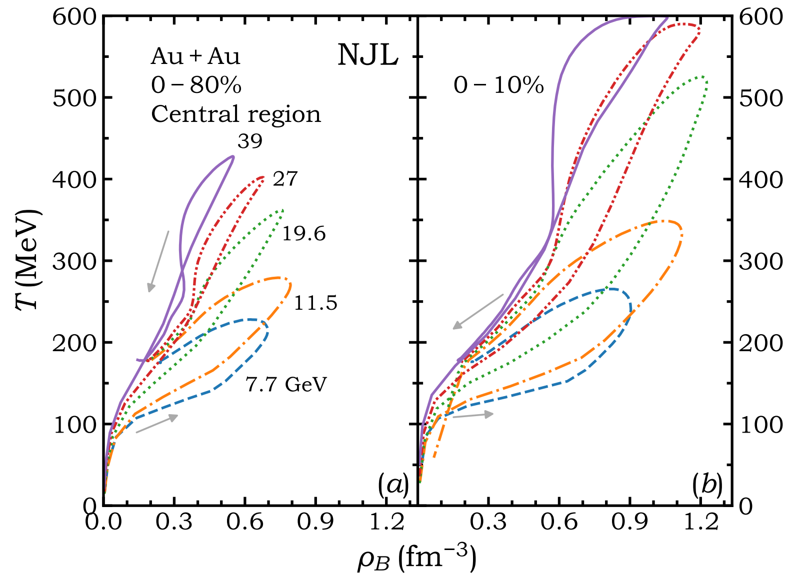

CME meets Machine Learning

- The CME-meter constructed shows high accuracy in recognizing the charge separation signal.
- A novel deep learning approach based on a U-Net architecture to time-reversely unfold CME dynamics is built to reconstruct the CME across the entire evolution of HICs.

Y. Zhao, L. Wang, K. Zhou, X. Huang Phys. Rev. C 106, L051901 (2022); S. Guo, L. Wang, K. Zhou, G. Ma, Chinese Phys. Lett. 42, 110101 (2025)

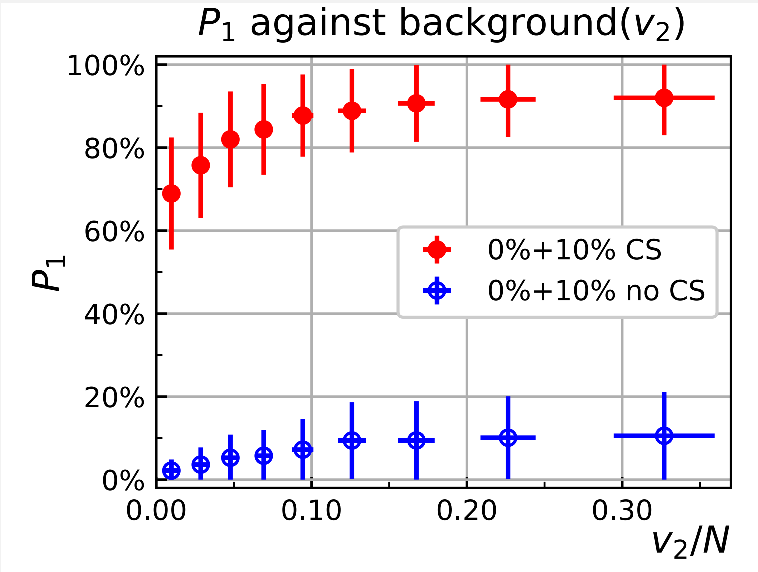

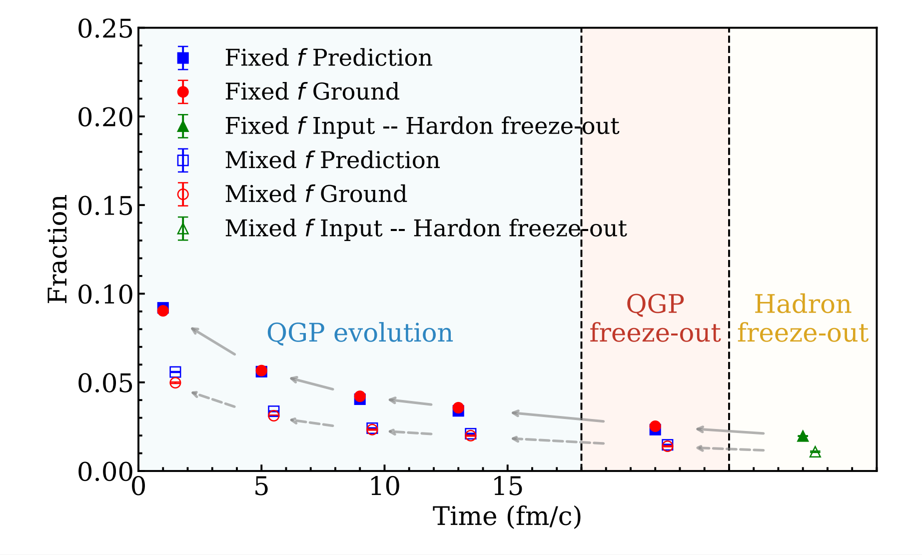

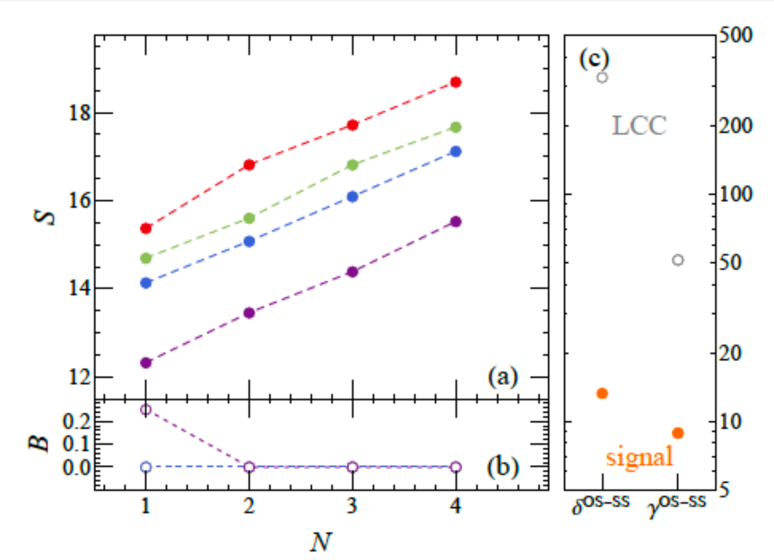

Y. Hirono, K. Ikeda, D. Kharzeev, Z. Liu, S. Shi, arXiv:2504.03248

- Optimal observables from ML, up to 90% higher sensitivity to CME signal than “standard” observables

$$S = \frac{f_c}{2}\left(\frac{O_{\mathrm{C,L}} - O_{\not\mathrm{C},\mathrm{L}}}{\sqrt{\frac{\Delta^2_{\mathrm{C,L}}+\Delta^2_{\not\mathrm{C},\mathrm{L}}}{N_{\mathrm{ev}}}}} + \frac{O_{\mathrm{C},\not\mathrm{L}} - O_{\not\mathrm{C},\not\mathrm{L}}}{\sqrt{\frac{\Delta^2_{\mathrm{C},\not\mathrm{L}}+\Delta^2_{\not\mathrm{C},\not\mathrm{L}}}{N_{\mathrm{ev}}}}}\right). \quad (7)$$

$$O = \sum_j X_j^{(\mathrm{L})}\, e_j + \sum_{j,j'} X_{j,j'}^{(\mathrm{E})}\, e_j\, e_{j'} + \sum_{j,j'} X_{j,j'}^{(\mathrm{O})}\, o_j\, o_{j'}\,. \quad (4)$$

$$B = \frac{1}{2}\left(\frac{O_{\mathrm{C,L}} - O_{\mathrm{C},\not\mathrm{L}}}{\sqrt{\frac{(\Delta^2_{\mathrm{C,L}}+\Delta^2_{\mathrm{C},\not\mathrm{L}})}{N_{\mathrm{ev}}}}} + \frac{O_{\not\mathrm{C},\mathrm{L}} - O_{\not\mathrm{C},\not\mathrm{L}}}{\sqrt{\frac{(\Delta^2_{\not\mathrm{C},\mathrm{L}}+\Delta^2_{\not\mathrm{C},\not\mathrm{L}})}{N_{\mathrm{ev}}}}}\right). \quad (8)$$

CME search with Event Shape Engineering

- Subtracted flow background by plotting $\Delta\gamma_{ESE}^{112}$ against v_2 within a given eccentricity (q_2) class in different rapidity bin.
- CME signal consistent with zero at 200 GeV.

H. S. Li for STAR Col., QM 2025, Initial Stage 2025

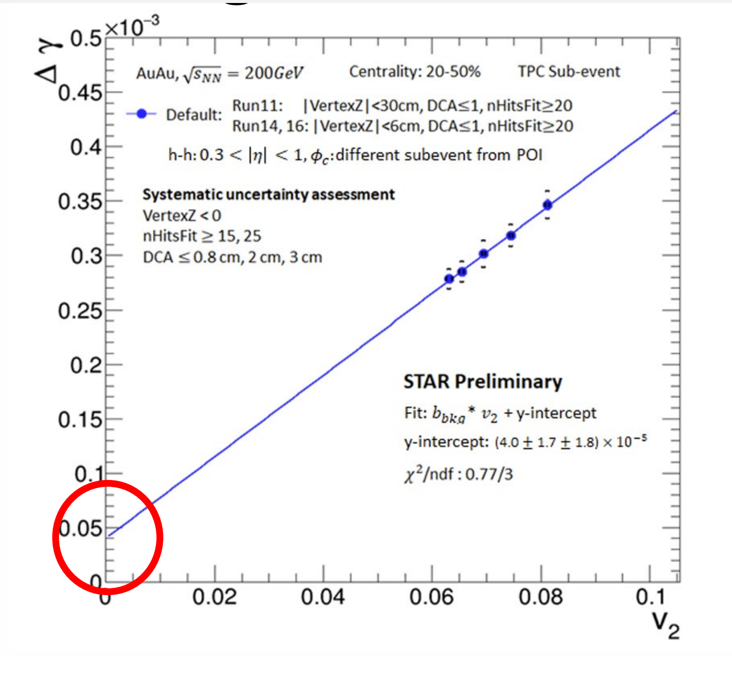

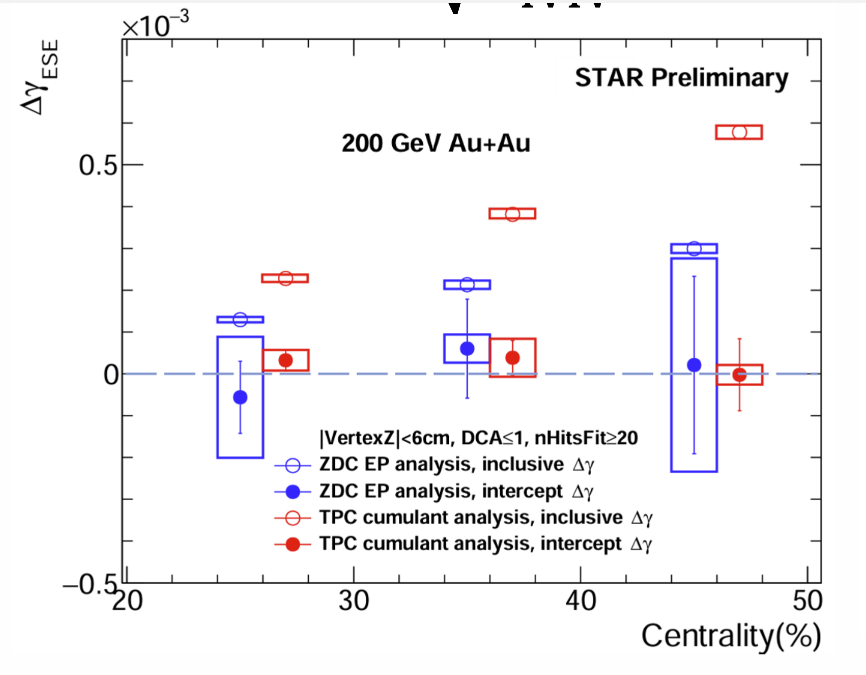

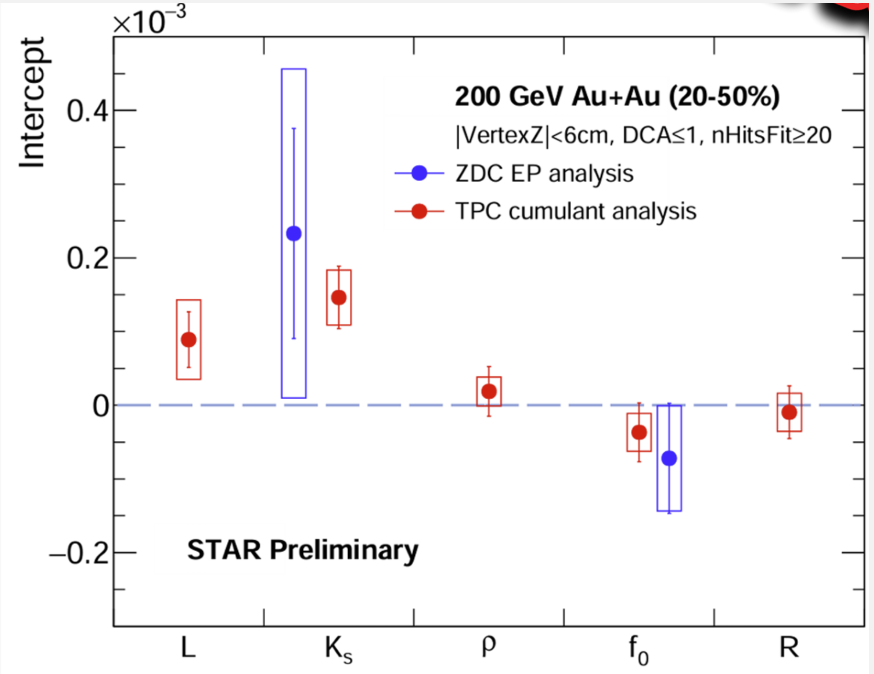

Updates from LHC, the PID CME

Z. Wang (ALICE) QM2025

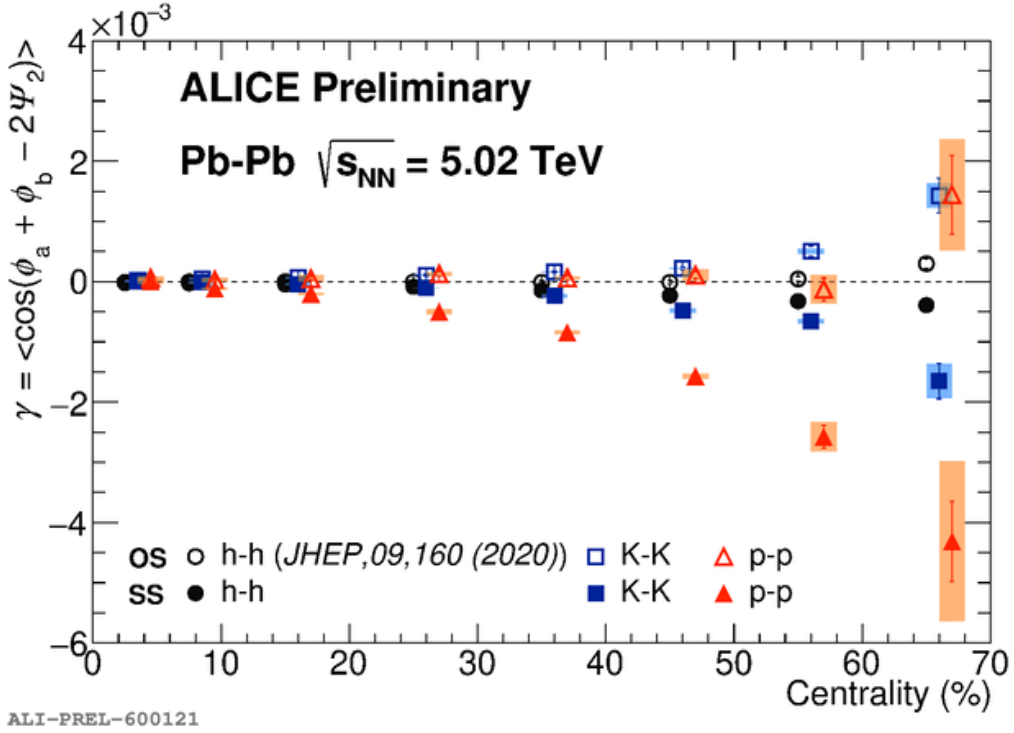

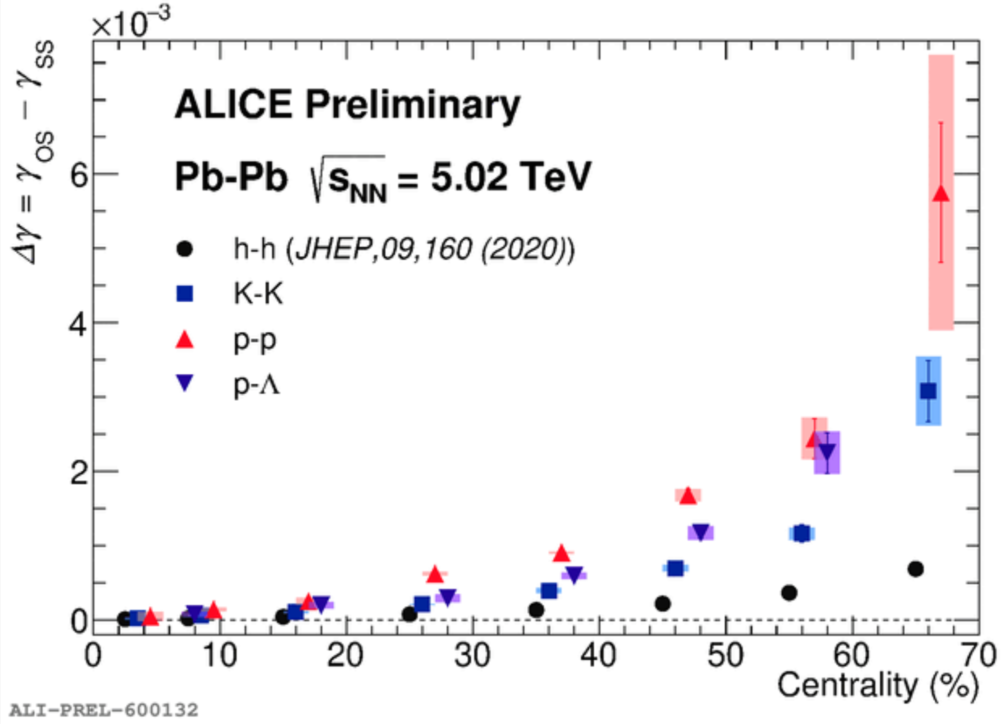

- Significant separations are observed for K and p, suggesting the existence of the charge-dependent correlations
- Δγ follow p-p > p-Λ > K-K > h-h
- Theoretical inputs are highly welcome to understand data: various (electric-, strangeness-, baryonic-)charge conservations + collectivity

Measurements of the CVE

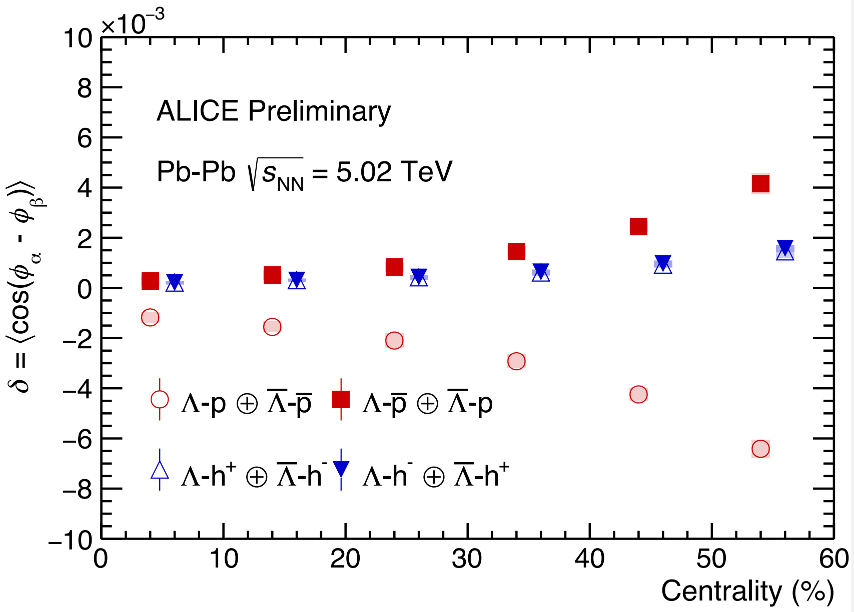

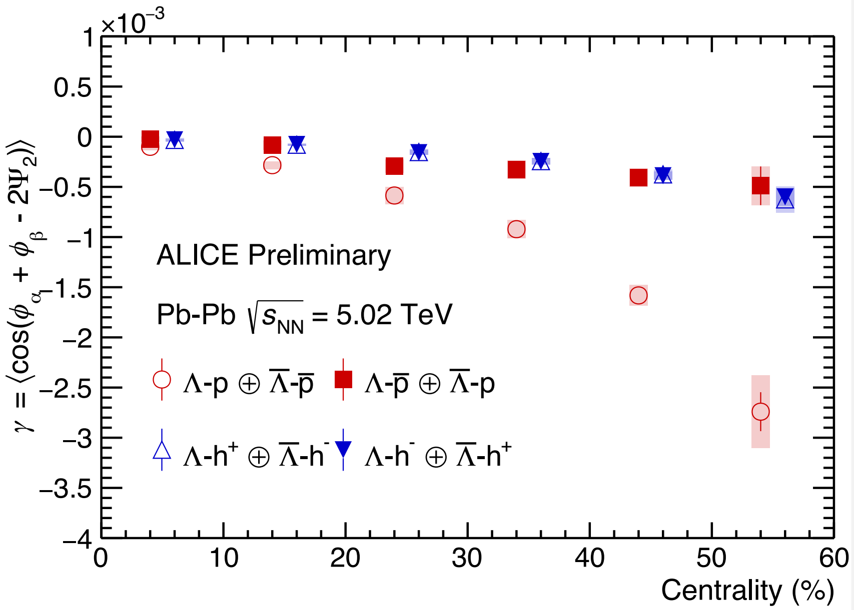

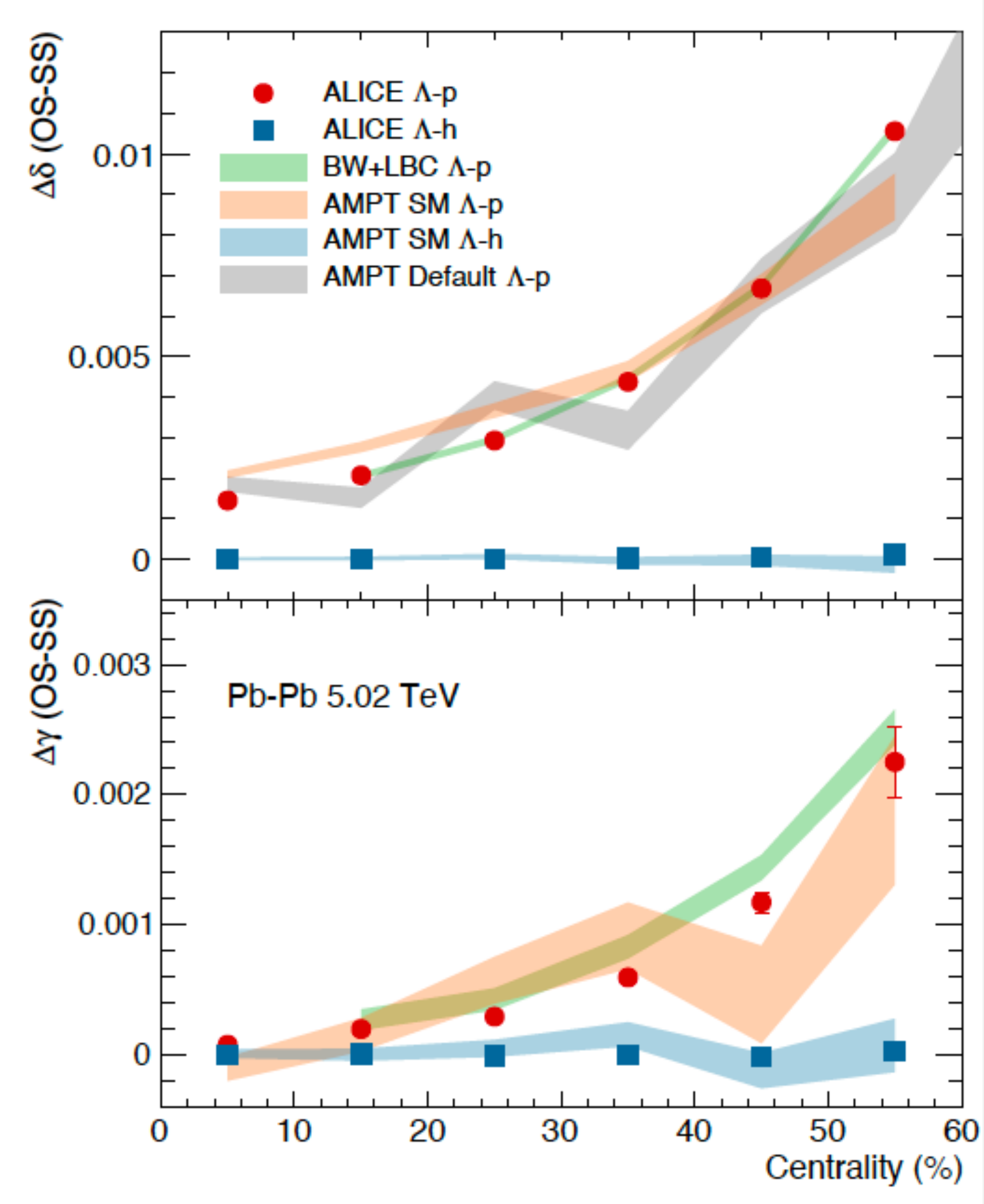

- δ and γ correlators of Λ–p show clear separations
- Can be partially interpreted by models, suggesting baryonic conservation + collectivity

C. Wang, J. Wan, J. Liao et al., arXiv: 2509.09025

Summary and Outlook

- The novel event shape selection effectively suppresses flow-related backgrounds
  - at 200 GeV, upper limit of f_{CME}~10%.
  - at each of 11.5, 14.6 and 19.6 GeV, a positively finite $\Delta\gamma_{ESS}^{112}$ (>3σ). Over 5σ if combined.
  - around 7.7 GeV, approaches zero CME limited with large uncertainties.

"The STAR CME result at lower RHIC energies is a major milestone in a 25+ year long quest for observing the effects of QCD topology. " Kharzeev at Chirality 2025

"While the results clearly indicate a significant charge separation in mid-central Au+Au collisions at 10--20 GeV, the current experimental approach cannot unambiguously identify the nature of the signal observed in $\Delta\gamma_{ESS}^{112}$. The zero value of $\Delta\gamma_{ESS}^{132}$ does not guarantee that $\Delta\gamma_{ESS}^{112}$ is free of residual background contributions. If future studies were able to further quantify the possible residual background and show it to be negligible, the present data would manifest an intriguing scenario where the chirality imbalance in quarks and the intense magnetic field coexist to trigger the CME." STAR arXiv:2506.00278

- Improve understanding background contributions

Acknowledgement

It is 25 years since first collisions at the Relativistic Heavy Ion Collider (6/12/2000)

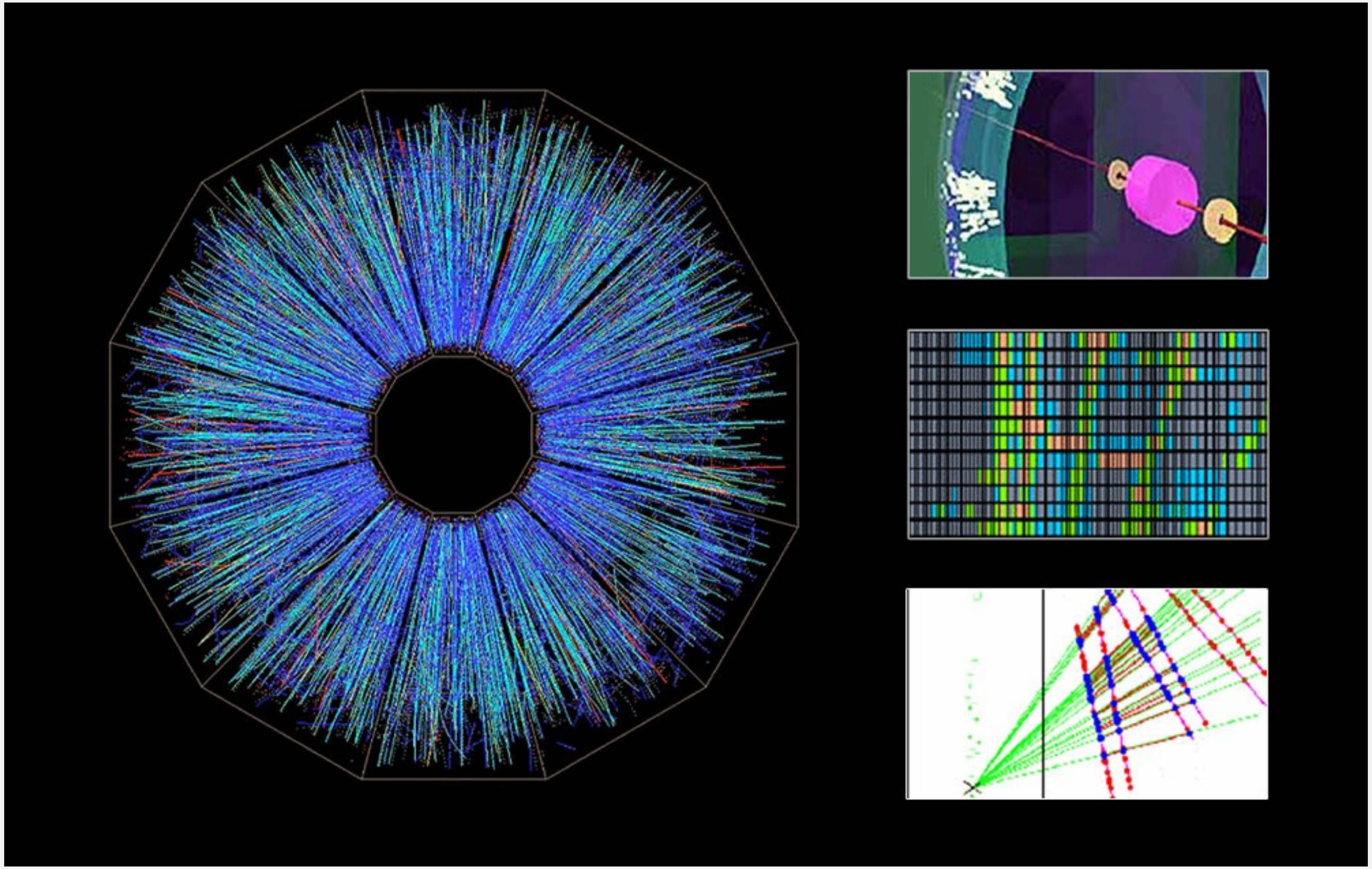

Thank you!

STAR 25-year celebration, 12/17-18/2025   https://indico.bnl.gov/event/29990